Flocculation of deep-sea clay from the Clarion Clipperton fracture zone

Ali, W.; Kirichek, A.; Chassagne, C.

DOI
10.1016/j.apor.2024.104099

Publication date
2024

Document Version
Final published version

Published in
Applied Ocean Research

Applied Ocean Research 150 (2024) 104099

Contents lists available at ScienceDirect

Applied Ocean Research

journal homepage: www.elsevier.com/locate/apor

Research paper

Flocculation of deep-sea clay from the Clarion Clipperton fracture zone

W. Ali [a,*], A. Kirichek [b], C. Chassagne [a]

[a] Section of Environmental Fluid Mechanics, Department of Hydraulic Engineering, Faculty of Civil Engineering and Geosciences, Delft University of Technology, Stevinweg 1, 2628 CN Delft, The Netherlands

[b] Section of Rivers, Ports, Waterways and Dredging Engineering, Department of Hydraulic Engineering, Faculty of Civil Engineering and Geosciences, Delft University of Technology, Stevinweg 1, 2628 CN Delft, The Netherlands

ARTICLE INFO

Keywords:
Deep sea mining
Organic matter
Cohesive sediment
Sediment plume
Turbidity flows
Particle size

ABSTRACT

This article discusses whether or to what extent flocculation plays a role in the saline deep-sea environment and whether sediment plumes generated by deep-sea mining activities are affected by the process of flocculation. The results of our laboratory study demonstrate that deep sea mineral clay with a median floc size of 20 μm can flocculate quickly within 2.5 min of mixing to form flocs with a median floc size of about 50–150 μm and outliers as large as 500 μm in size due to the presence of natural organic matter. At high shear (turbulent mixing), a threshold of about 125 s^{-1} was found above which, organic matter can successfully bind to clay. Above 125 s^{-1}, the steady-state floc size is also found to increase linearly with shear. In low energetic conditions (when flocs experience mainly differential settling), the median floc sizes are found to be 2 or 3 times larger than at turbulent mixing. As expected, the rate of flocculation is greater at higher clay concentrations. At long mixing times, the median floc size is found to decrease due to the breaking/reconformation of flocs. Experiments performed to study the ageing of flocs at rest demonstrated that a dynamic process was ongoing between the organic matter and the clay. It is hypothesized that the organic matter present has amphiphilic properties. Over time, the organic matter would rearrange itself such as to maximize its contact area with the mineral clay, resulting in two effects, depending on the structure of the flocs. In the case of flocs formed at high shear, it led to a rupture of flocs. A slow agitation of settled flocs, having previously experienced low shear conditions, on the other hand, led to aggregation. Overall, the results found in the present article show that flocculation likely plays a significant role in deep-sea areas.

1. Introduction

Flocs are widely found in coastal environments, and their presence significantly impacts sediment transport (Gratiot and Manning, 2004; Deng et al., 2019; Safar et al., 2019; Ho et al., 2022). It was found that flocculation occurs rapidly when coastal environment conditions are recreated in the lab (in terms of salinity and shear), often taking only a few minutes, especially when microscopic organic matter is present (Gillard et al., 2019; Shakeel et al., 2020). In the marine and coastal systems, particle aggregation and break-up are ongoing dynamic processes influenced by changes in shear, salinity and type and amount of organic matter. Below the permanent thermocline in the ocean interior, where currents are significantly weakened, the dominant process driving particle aggregation at these low shears is differential settling, which leads to the formation of large flocs known as marine snow (Alldredge and Silver, 1988). Marine snow is mainly composed of organic matter, such as dead phytoplankton, faecal matter, and natural polymers produced by bacteria and phytoplankton. Most parts of marine snow are consumed by filter-feeding animals within the first 1,000 metres of their sinking. As sunlight cannot reach deep-sea organisms, they rely principally on marine snow as an energy source. Some unconsumed material, however, can reach the sea floor and become incorporated into the ocean bottom, where it is further decomposed through biological activity. At the sea floor a large microbial community is also found (Riemann, 1983; Verlaan and Cronan, 2022; Sujith and Gonsalves, 2021). The major component of these microorganisms and their excretions are marine phospholipids (Suzumura, 2005). Deep-sea environments cover 65% of Earth's surface and host 95% of the global biosphere, yet remain largely unknown as only 0.001% of their biodiversity has been sampled and described (Gage and Tyler, 1991; Danovaro et al., 2008; Webb et al., 2010). The composition of the sediments in these regions differs depending on the location and formation factors. Typically, Clarion Clipperton Fracture Zone (CCFZ), contains clay, silt, sand, rock fragments, and organic material (BGR, 2019; Lang et al., 2019; Zawadzki et al., 2020). The

* Corresponding author.
E-mail address: w.ali@tudelft.nl (W. Ali).

https://doi.org/10.1016/j.apor.2024.104099
Received 15 December 2023; Received in revised form 2 May 2024; Accepted 17 June 2024
Available online 27 June 2024

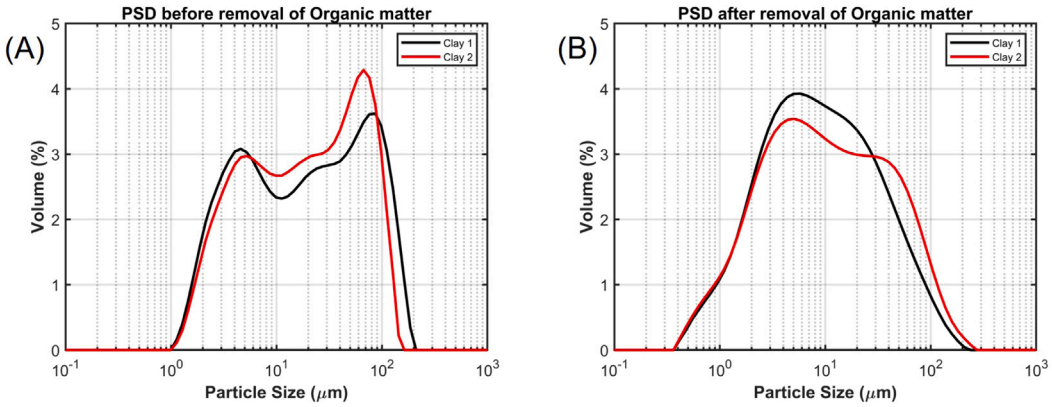

Fig. 1. PSD of Clay 1 and Clay 2 collected from CCFZ. (A) Shows the PSD before the removal of organic matter, whereas (B) shows PSD after the removal of organic matter.

deep-sea environment is typically favourable for flocculation due to its elevated salinity and substantial organic matter concentration (Mewes et al., 2014; ISA, 2015; Fettweis and Baeye, 2015; Volz et al., 2018).

The abyssal plains of the deep sea also possess vast reserves of polymetallic nodules, in certain areas, which, unlike on land, comprise a range of metals in a single deposit. In the CCFZ, a large area abundant in these nodules, cobalt, nickel, copper, and manganese, are all present in a single ore (ISA, 2019; Harbour et al., 2020; Hein et al., 2020). There is at present a high demand for metals, such as manganese, nickel, and cobalt, which are necessary for the manufacture of wind turbines, solar panels, and batteries for electric cars (Hein et al., 2020). While these metals are typically extracted through land-based mining, deep-sea mining is being viewed as a possible alternative to satisfy the growing demand. However, it is crucial to recognize the environmental consequences of the associated dredging operations, which have the ability to disrupt benthic ecosystems and produce sediment plumes with a high concentration of suspended solids (Kaiser et al., 2013; Peacock and Alford, 2018).

The nodule mining procedures involve the usage of the Seafloor Mining Tool (SMT), which gathers nodules from the seafloor and separates them from unnecessary water and sediments. During this process, the leftover water and sediment are discharged behind the mining vehicle on the seafloor. The generation of turbidity currents within the near-field region is a particular worry in this mining operation. Various flow regimes, including jets, plumes, and turbidity currents corresponding to the ones generated by the SMT have been studied (Elerian et al., 2022; Peacock and Ouillon, 2023; Ali et al., 2022; Blue Nodules D1.7, 2020; Hein et al., 2020; Haalboom et al., 2022). They found that the generated currents may remain suspended for extended periods (Gillard, 2019; Blue Nodules D1.7, 2020; Hein et al., 2020; Haalboom et al., 2022). Their settling and subsequent smothering effect can result in the burial of benthic species, hindrance of respiratory surfaces for filter feeders, and contamination of food sources for numerous benthic organisms (Vanreusel et al., 2016; Gollner et al., 2017; Jones et al., 2017).

When studying the propagation of turbidity currents, it was found that flocculation indeed occurs during the propagation of the sediment (Ali et al., 2022), thanks to the fast flocculation kinetics resulting from organic matter–clay interactions. This flocculation significantly impacts the propagation of turbidity currents and sediment plumes (Elerian, 2023). In the context of deep-sea clay, the work done by Gillard et al. (2019) showed that at a low shear rate, at a concentration of 0.5 $g\,L^{-1}$ deep sea clay is flocculating. There is, however, not yet any data available for a wide range of deep-sea clay concentration and shear rates, which are representative of the shear rates, mixing times and concentrations found during mining operations.

The aim of the present study is, therefore, to explore the changes in the particle size distribution of clays representative of deep sea mining locations (CCFZ), as a function of various clay concentrations, mixing times, and shear rates. Note that the experiments are performed at regular atmospheric pressure (10^5 Pa). The pressure in the deep sea is about 400 times higher. However, neither mineral sediment nor organic matter is expected to behave differently, considering the fact that mineral sediment has an incompressible crystalline structure and that organic matter is mainly composed of polyelectrolytes (stemming from phytodetritus) similarly indifferent to pressure. We will show that our results indeed match the results of Gillard et al. (2019) who performed flocculation studies at deep sea pressures. A series of flocculation experiments were conducted using jars, with variations in mixing times, clay concentrations, and shear rates. The influence of the flocs' residence time at the bottom of the jars was also studied. In addition, flocculation experiments at very low shear, resulting in differential settling, were conducted in a novel rotating wheel setup. Particle sizes and their associated settling velocities were measured using an in-house video microscopy set-up coupled with a settling column.

The article is structured as follows: materials used and the experimental setups are given in Section 2. Results and discussions are presented in Section 3. Finally, conclusions are summarized in Section 4.

2. Material and methods

2.1. Clay

Two types of clay were used for the experiments; each was collected from a different area of the CCFZ at a water depth of approximately 4000 metres. For convenience, we refer to them as Clay 1 and Clay 2. Clay 1 was collected from the German licensing area of CCFZ, while Clay 2 was collected from the NORI-D area of CCFZ. Both types of clay were stored in a refrigerator (at 6 °C). The total organic carbon (TOC) was calculated from the difference between total carbon (TC) and total inorganic carbon (TIC). The TC was measured by utilizing a UNICUBE device made by Elementar Analysensysteme GmbH, while TIC was determined by gas chromatography and acid digestion. TOC in Clay 1 is approximately 0.53 wt%, and for Clay 2 is 0.55 wt%. The TOC values align with those observed in previous research conducted in the CCFZ region (BGR, 2019). The type of organic matter in Clay 2 visually differed from Clay 1. Clay 2 organic matter seems to be composed of long elongated strings, whereas Clay 1 organic matter did not display such strings. The Clay 1 and Clay 2 samples have a d_{50} around 20 μm, determined through static light scattering, using a Malvern Master Sizer 2000 (Ali and Chassagne, 2022). The Particle size distribution (PSD) before and after the removal (by using the loss on ignition method: sample heating for 5 h at 600 °C) of organic matter can be found in Fig. 1. Both Clay 1 and Clay 2 were used as received, implying that no organic matter was removed from the samples.

2.2. Flocculation experiments

The flocculation experiments were carried out at ambient pressure (10^5 Pa) and room temperature (21 °C) with different clay concentrations and mixing times. The measurements were performed in a JLT6 jar setup provided by VELP Scientifica, Italy. The jars have dimensions of 95 mm in diameter and 110 mm in height. To stir each suspension, a rectangular paddle was used, measuring 25 mm in height and 75 mm in diameter. The paddle was positioned 10 mm above the bottom of the jar within the suspension. The shear rate employed for the flocculation experiments remained constant at 50 s^{-1}, and the clay was mixed in saline water, having a salinity of 34.68 PSU, which is equivalent to the average salinity of the ocean water. For practical reasons, the saline water was made using NaCl salt (analytical grade, provided by Boom Laboratorium, The Netherlands) and tap water (Table 1 in supplementary material shows the properties of the tap water used), and some flocculation tests with artificial seawater showed that the results presented in the article are representative of seawater conditions. Gillard et al. (2019) studied flocculation using saline water from the CCZ region and found similar results. Other tests showed that the clays did not flocculate in tap water, which highlights the role of salt in flocculation. All clays were fully dispersed in saline water before the measurements, as the clay received was in the form of a compact, fully saturated lump (see Figure S1). To ensure a full dispersion, the required amount of clay was taken from the lump and put in a jar. Then, saline water was added to achieve the desired concentration. The full dispersion of the clay was achieved using a high-stirring mixer with a speed of about 600 RPM for 60 min. This protocol was used for all experiments presented in this article.

Based on the amount of clay available for experiments, for Clay 1, five different concentrations (0.5, 1.0, 1.5, 2.0, and 5.0 g L^{-1}) were used. Regarding Clay 1, experiments were performed at seven different mixing times (2.5, 5, 10, 30, 60, 90, and 120 min). For Clay 2, three concentrations (0.5, 2.0, and 5.0 g L^{-1}) and four mixing times were used (2.5, 30, 60, and 120 min). After mixing, the paddle rotation was stopped, and flocs were left to settle to the bottom of the jar for about one hour. The flocs were then carefully collected using a pipette and deposited at the top of the settling column used in the FLOCCAM set-up. When collecting samples, a modified pipette with a 50 mL capacity and a 3 mm diameter was employed to extract a sub-sample of floc from the jar with great care. The sub-sample was then transferred directly to the settling chamber of the FLOCCAM, where the aperture of the pipette was in contact with the column water surface. This allowed the flocs to settle naturally and unaided, purely under the influence of gravity. Floc sizes and their corresponding settling velocities were then measured using the FLOCCAM equipment described below.

2.3. FLOCCAM

The FLOCCAM set-up consists of a rectangular settling column and uses video microscopy to measure particle size distribution (PSD) for particles larger than 20 µm and their settling velocities (Manning et al., 2007; Ye et al., 2020; Shakeel et al., 2021; Ali et al., 2022, 2023). The settling column has dimensions of 10 cm x 10 cm x 30 cm, featuring glass panels on the front and rear, with plastic sides. The camera utilized is a 5MP CMOS camera with a resolution of 2592 x 2048 pixels, 4.8-micrometre pixel size, and a Global Shutter, identified as iDS UI-3180CP-M-GL Rev.2.1 (AB02546). The camera is equipped with the S5VPJ2898 telecentric lens featuring a tunable working distance and a C-mount, produced by Sill Optics GmbH & Co. KG. Fig. 3(A) illustrates the equipment set up in a schematic representation. The Safas software package was employed to analyse recorded videos of settling flocs in a settling column, allowing for the calculation of the flocs' PSD, shape, and settling velocity (MacIver, 2019).

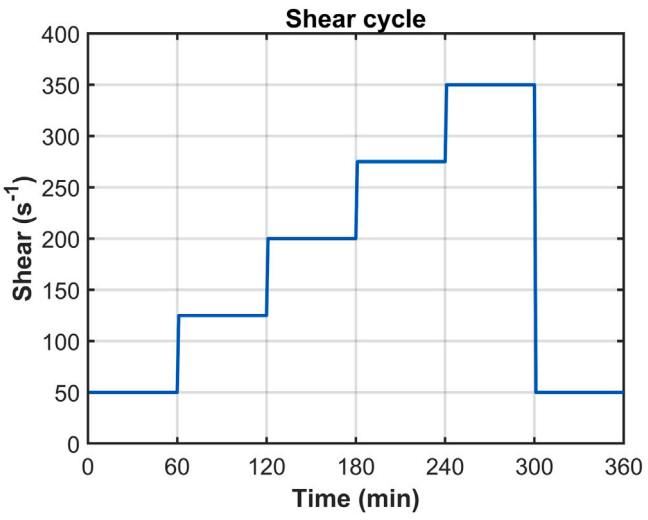

Fig. 2. Schematic showing shear cycle experiment process.

2.4. Shear cycle experiments

Shear cycle experiments were conducted in order to investigate the influence of shear rate on the median floc size. Six shear rates (50, 125, 200, 275, 350 and 50 s^{-1}) were used in the shear cycle experiment as shown in Fig. 2 for 5 g L^{-1}. Each shear step had a duration of 60 min to ensure that a steady-state floc size has been reached at the end of the step.

2.5. Residence time at the bottom of the jar

Experiments were conducted to study the influence of the residence time of flocs at the bottom of the jar on their size. For Clay 1, various concentrations (0.5, 1.0, 1.5, 2.0, and 5.0 g L^{-1}) were tested. The samples were flocculated in the jar for a duration of 1 h and then placed in a refrigerator at a temperature of 6 °C. The size of the flocs (collected from the bottom of the jar) was measured on days 1, 2, 10, and 30. Regarding Clay 2, two experiments were performed at a concentration of 0.5 g L^{-1}. One jar was placed in the refrigerator at a temperature of 6 °C, while the other jar was kept at room temperature (21 °C). The size of the flocs (collected from the bottom of the jar) was measured on days 1, 2, 10, and 30.

2.6. Rotating wheel

Experiments in a novel in-house set-up, known as a rotating wheel (Fig. 3(B)) were conducted to induce flocculation at low shear. The rotating wheel experiments were conducted with Clay 1 at a shear rate of 1 s^{-1}. The inner diameter of the wheel is 34 cm with a depth of 7 cm. The wheel was filled up to the top with suspension for all experiments. Three concentrations were considered (0.5, 2.0, and 5.0 g L^{-1}) with four mixing times (2.5, 30, 60, and 120 min). Floc size measurements of flocs created in the wheel and their corresponding settling velocities were also calculated after 2, 10, 20, and 30 days.

3. Results and discussion

3.1. Influence of mixing time and concentration

The effect of mixing time and clay concentration on flocculation are given in Fig. 4. The median floc size for Clay 1 is compared with the median floc size of Clay 2 for different concentrations and mixing times, and it is clear that Clay 2 flocculates much faster than Clay 1

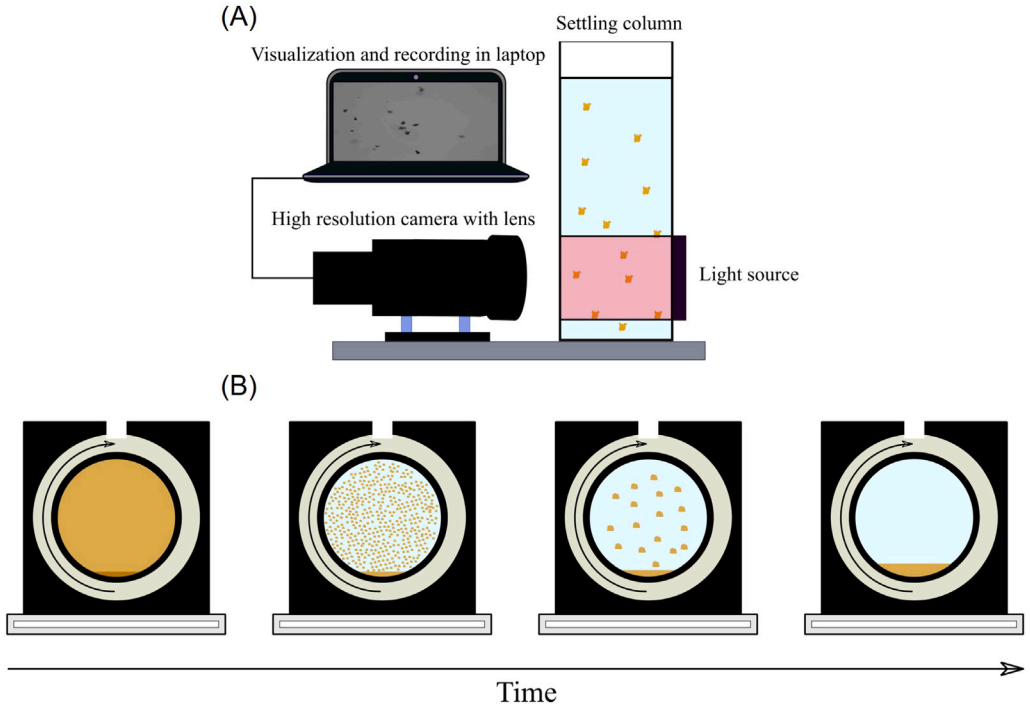

Fig. 3. (A) Schematic representation of the FLOCCAM setup (Ali et al., 2022). (B) Schematic representation of the rotating wheel setup and experimental procedure: the dispersed clay is mixed slowly in the rotating wheel, and flocculation occurs over time. At the end of the experiment, the rotation is stopped, and samples are collected from the settled material.

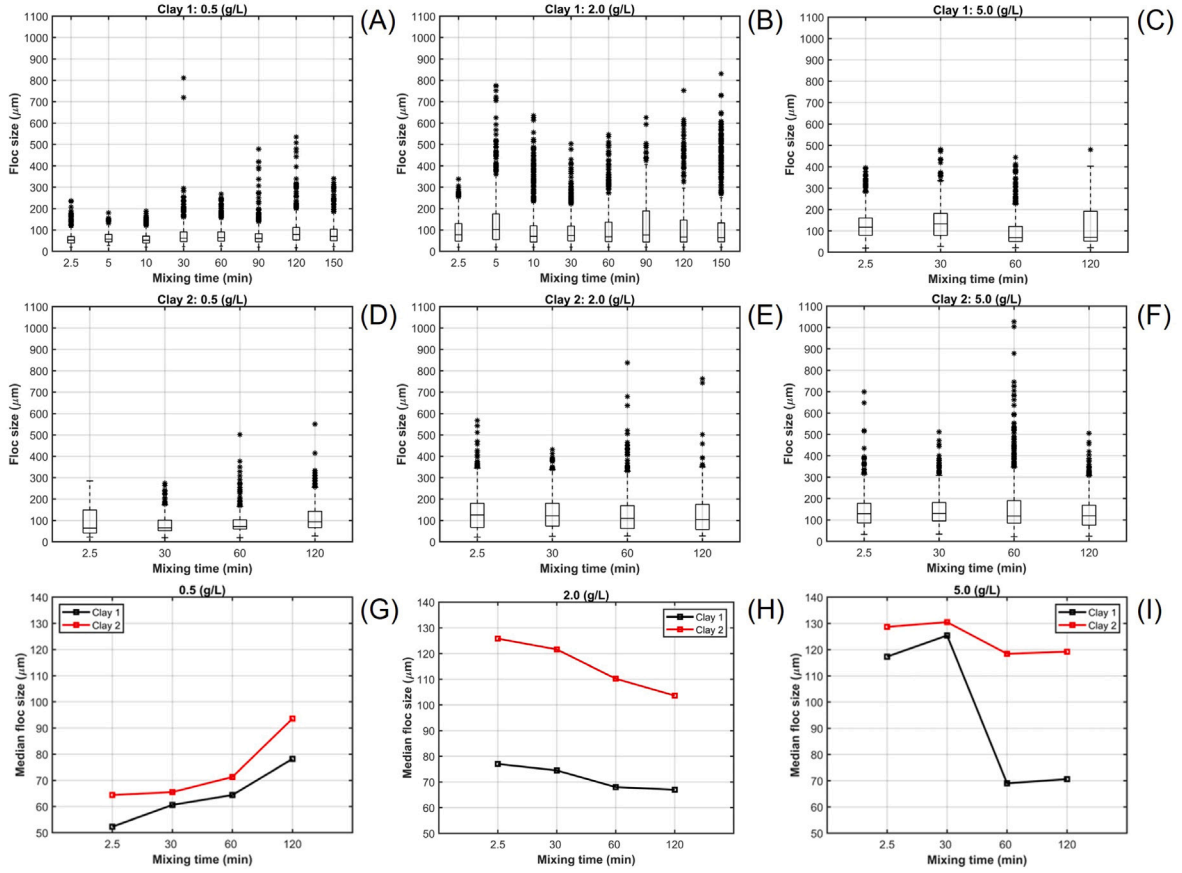

Fig. 4. Effect of mixing time on flocculation of Clay 1 (A–C) and Clay 2 (D–F) concentrations of (A, D) 0.5 g L^{-1}, (B, E) 2.0 g L^{-1} and (C, F) 5.0 g L^{-1}. Median floc size for Clay 1 and Clay 2 concentrations of (G) 0.5 g L^{-1}, (H) 2.0 g L^{-1} and (I) 5.0 g L^{-1}.

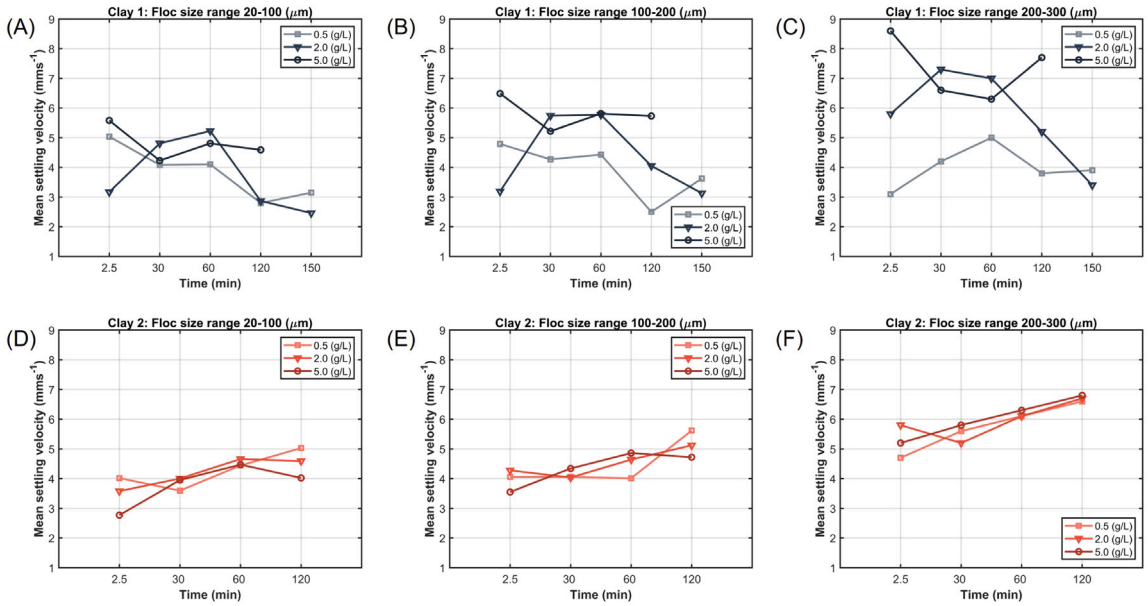

Fig. 5. Mean settling velocity of flocs for different floc size ranges, concentrations and time for Clay 1 flocs (A–C), Clay 2 flocs (D–F).

and has a higher median floc size in all cases (see Fig. 4(G-I)). This can be attributed to the type of organic matter content in Clay 2 since organic matter is one of the main drivers for flocculation for natural sediments (Kranck, 1973; Mietta et al., 2009; Deng et al., 2019; Lee et al., 2019). Moreover, it has been observed that at low concentration, $0.5\,g\,L^{-1}$, (see Fig. 4(G)), the floc size of both clays increases with increasing mixing time, whereas for higher concentrations, the floc size decreases with increasing time (see Fig. 4(H, I)). Fig. 4 shows that at $0.5\,g\,L^{-1}$, the size of the outliers increases over time (up to 120 min), and from visual inspection we can confirm that the flocs formed are open and have the large structure. At 150 min of mixing time, both the median size and the size of the outliers (that was only measured for Clay 1) are smaller than at 120 min. Furthermore, for Clay 1 at $2.0\,g\,L^{-1}$, the median size of flocs and the size of the outliers increase significantly between 2.5 and 5 min. After 5 min of mixing, the median floc size decreases with mixing time. This rapid growth, followed by a size decay, was already observed for clay flocculated using (cationic) polyelectrolyte (Shakeel et al., 2020). A characteristic size is given by the Kolmogorov microscale, which, for the shear rate used in the experiments (about $50\,s^{-1}$), is of the order of 150–200 μm. Flocs having a size well below this range (as is the case for the $0.5\,g\,L^{-1}$ experiments until about 100 min of mixing) can grow in time. Flocs having a size well above this range (as is the case for the experiments done at higher clay concentrations and for $0.5\,g\,L^{-1}$ experiments above 100 min of mixing) reconform or are eroded over time due to the experienced shear (Dyer, 1989; Deng, 2022).

It is also observed that Clay 1 and Clay 2 outliers have their size decreasing with mixing time until about 30 min of mixing, which is in line with the fact that the size of these outliers is well above the 150–200 μm size range estimated above. These outliers are, therefore, either reconforming or being eroded over time. After 30 min of mixing, however, the size of outliers is increasing again. The reason for this increase is related to an increase in "double flocs" (flocs made of two flocs attached together). Some of these double flocs are shown in supplementary material (see Figure S2).

The mean settling velocities of flocs for different floc size ranges, concentrations and times are given in Fig. 5. As detailed in Ali et al. (2023), the measured settling velocities cannot be straightforwardly related to the Stokes settling velocity of flocs, as flocs usually fall in the wake of other flocs, which significantly influence the local hydrodynamics. We note that the mean settling velocity of flocs is clearly increasing with mixing time for all concentrations for Clay 2 flocs. No such trend can be observed for Clay 1 flocs, but the mean settling velocity is generally higher than for Clay 2 flocs. As Clay 2 flocs have an organic matter that differs from Clay 1 flocs, they are probably more prone to reconformation than Clay 1 flocs. Therefore, their density will increase with increasing shearing, which explains why their settling velocity increases with mixing time. Clay 1 flocs have a higher overall density and, therefore, a higher settling velocity than Clay 2 flocs. The effect of floc reconformation is probably limited for Clay 1. For $2.0\,g\,L^{-1}$, while the mean floc size decreases with mixing time, the average settling velocity increases for all size ranges until 60 min of mixing, which is consistent with a reconformation and compaction of flocs. In contrast, the average settling velocity of Clay 1 flocs for all size ranges decreases overall for mixing times of more than 60 min. In particular, the fact that flocs in the 20–100 μm size range have a decreasing settling velocity with mixing time would agree with an erosion of flocs, whereby the eroded 20–100 μm flocs have a higher organic matter content than the original unflocculated 20–100 μm clay particles.

Analysing the video microscopy data for the highest Clay 1 concentration, 2 and 5 g/L, it became clear that there was a complicating factor in the estimation of settling velocities, as long organic matter strings or swirls (see Figures S2 and S3) were observed in the videos. Clay particles could, therefore, experience sweep flocculation and be embedded in these long strings, which might also erode or break over time, contributing to lower settling velocities in each size range. Our flocculation experiments at room temperature and pressure for both clays lead to floc sizes that are comparable to the ones measured by Gillard et al. (2019), at deep sea representative conditions.

3.2. Shear cycle experiments

The floc size distribution and median floc size for both Clay 1 and 2 are shown in Fig. 6. Both clays show similar behaviour of median steady-state floc size as a function of shear. Due to differences in the type of organic matter, the Clay 2 floc sizes are always larger than the Clay 1 floc sizes. For both clays, it is observed that after the first shear step, the steady-state floc size decreases and then increases with increasing shear. The median floc size at $50\,s^{-1}$ shear is the same before and after the shear cycle (see the green points in Fig. 6(C), which symbolizes the $50\,s^{-1}$ floc size measured at the end of the shear cycle).

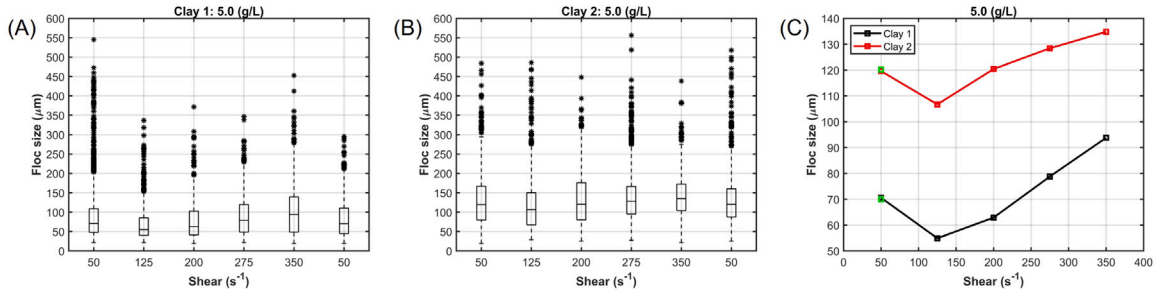

Fig. 6. Effect of the shear cycle on floc size of Clay 1 (A) and Clay (B). Comparison of median floc size changes during the shear cycle in Clay 1 and 2 (C). The green point represents the values of median floc size at shear $50\,s^{-1}$ at the end of the shear cycle.

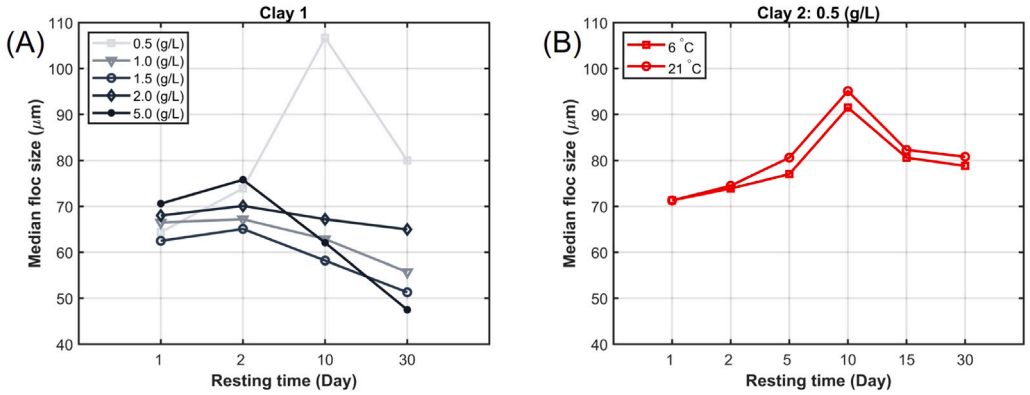

Fig. 7. Effect of resting time of median floc size: (A) for Clay 1 at different concentrations and (B) for different temperatures.

For Clay 1, however, it is observed that the size of the outliers after the shear cycle is smaller compared to the beginning of the shear cycle. For Clay 2, there is no significant change in outlier size.

Previous studies show that a decrease in median floc size with shear is usually observed in shear experiments (Shakeel et al., 2020; Ali and Chassagne, 2022). When performing shear cycle experiments, it is found that the floc size is either reversible or non-reversible depending on the forces between the constituents of the flocs. If the interaction forces are weak enough, such as between anionic polyelectrolytes and negatively charged clay particles, the floc size is reversible as a stationary floc size is found for each shear rate (Shakeel et al., 2020). When the interaction is stronger, as is the case for flocs formed by cationic polyelectrolytes and negatively charged clay particles, flocs are irreversibly broken at high shear. This implies that, depending on the history of such a floc, different floc sizes can be found: A floc formed at low shear will usually be large, and if this floc has later been subjected to high shear and break, it will never regrow to this large size when the shear is again lowered.

In the flocs studied here, the stationary floc size increases with the shear rate after $125\,s^{-1}$. This contradicts the expected behaviour, which is a decrease in size with the shear rate. We ascribe this peculiar behaviour to the specific type of organic matter in the samples. In the samples, we could observe organic matter polymeric strings that, over time, would bind to mineral clay or already flocculated material. In contrast to polyelectrolytes used as flocculant, which have very fast flocculation kinetics, it would seem that the organic matter present in the samples has slow flocculation kinetics. As shown in Fig. 1, both Clay 1 and Clay 2 flocs contain a small amount of organic matter. However, the amount of organic matter bound or unbound to clay is unknown. We hypothesize that at a higher shear, the interactions between organic matter and mineral clay or between organic matter and flocs are enhanced, and therefore, the flocculation kinetics is promoted compared to a lower shear. At the same time, the decrease in median floc size observed between $50\,s^{-1}$ and $125\,s^{-1}$ and the fact that the steady-state size at $50\,s^{-1}$ at the end of the cycle is the same as the one found at the beginning of the cycle suggests that there is another mechanism at stake. This suggests that organic matter has a low affinity for both water and mineral clay, implying that at low shear, flocculation is prevented and explains why the steady-state size is decreasing between $50\,s^{-1}$ and $125\,s^{-1}$. At these low shears, the hydrophobic organic matter would be in a state of coiling that does not promote flocculation. At $125\,s^{-1}$, break-up (erosion of flocs) and/or reconformation of flocs lead to a smaller steady-state floc size. At higher shear rates, the organic matter uncoils, and aggregation is promoted. If our hypothesis is correct, it would mean that the steady-state size reached at each shear step is to be found by a balance between aggregation and break-up rates. The aggregation rate would be proportional to the collision frequency, which is increasing with shear and a small collision efficiency that would be shear-dependent (the collision efficiency being close to zero below $125\,s^{-1}$). The break-up rate would be more weakly dependent on shear than the aggregation rate since the median floc size increases steeply with shear.

3.2.1. *Influence of residence time at the bottom of the jar*

Fig. 7 shows the median floc size for Clay 1 and Clay 2 presented as a function of the time that flocs have been resting at the bottom of the jars. For Clay 1, it is found for all concentrations except $0.5\,g\,L^{-1}$ that the median floc size decreases slightly as a function of resting time. For $0.5\,g\,L^{-1}$ of Clay 1 and for all experiments with Clay 2 at the same concentration, an increase in floc size is observed until day 10, followed by a decrease in size. From the experiments with Clay 2, it is concluded that temperature does not play a role in the observed trends, and therefore, neither does biological activity (which is temperature dependent).

It was observed while manipulating the jars containing the $0.5\,g\,L^{-1}$ samples that flocs were not in contact with each other while resting but that the slightest movement induced flocculation, as flocs would roll, getting in contact with each other. The protocol for sampling the flocs was identical for all samples, so the small perturbations induced

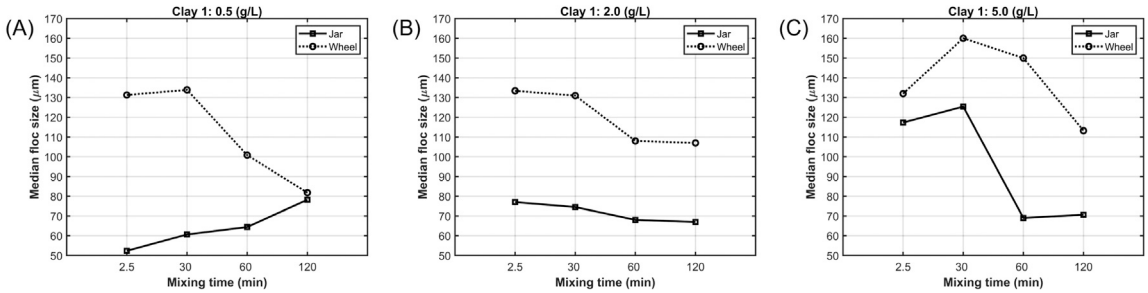

Fig. 8. Effect of mixing time on flocculation in the jar and the wheel for different concentrations: (A) $0.5\,g\,L^{-1}$, (B) $2.0\,g\,L^{-1}$ and (C) $5.0\,g\,L^{-1}$.

by the unavoidable handling of the jar and pipetting are expected to be the same for all samples. This is confirmed by the fact that all $0.5\,g\,L^{-1}$ experiments are consistent. Until day 10, it would appear that the organic matter promotes a very rapid flocculation, as the handling of the jar is happening for a few minutes only. After day 10, breaking and/or reconformation of flocs is occurring. At concentrations above $0.5\,g\,L^{-1}$, resting flocs are always in contact with each other at the bottom of the jars (see Figure S4). If our hypothesis of the low affinity between organic matter and water is confirmed, it would imply that there is a structural energy benefit for organic matter to bind with clay at the moment two flocs are put into contact. On the other hand, when the flocs are in contact while resting at the bottom of the jar, the increase in size is minimal (though apparent, see day 2 for Clay 1 in Fig. 7(A)). At longer times (after day 2 in all cases), the median floc size decreases with resting time. It could be that the organic matter at that time, through a slow diffusion process, has been rearranging itself around the mineral clay particles in such a way as to minimize contact with water. This would lead to a breakage of flocs so as to increase the available clay surface area for the organic matter. Substances, like phospholipids, which are key components of cell membranes and are found in the deep sea (Parzanini et al., 2018), are a class of lipids that are amphiphilic (having a hydrophilic "head" containing a phosphate group and two hydrophobic "tails" derived from fatty acids). The properties of the organic matter in our samples (low affinity for water, high affinity for clay) would hint at the fact that it is amphiphilic, like a phospholipid.

3.2.2. Flocculation in the wheel compared to jar experiment

Experiments with the wheel have been performed with Clay 1 only. During the slow rotation of the wheel, it was observed that the flocs residing at the bottom of the cylindrical wheel were entrained along the wheel wall and, at a position of about 135 degrees, would fall back to the bottom of the wheel (see Figure S5). At the same time, due to the sliding of particles along the wheel wall, particles at the bottom of the wheel were disturbing the deposited flocs and led to erosion of the finer particles in the direction opposite to the rotation. This continuing process led to full dispersion of the clay material in the wheel, making the water homogeneously turbid in the wheel, except for a layer of clay at the bottom of the wheel. The hydrodynamics in the wheel were, therefore, quite different from the ones in the jar, where most of the material was always suspended (with the exception of some heavy sand and silt particles) and experienced turbulent mixing. In contrast to jar test experiments, the shear in the wheel is very small and differential settling is expected to play a role in the experiments as the material is continuously entrained along or close to the wheel wall and falls down when gravity starts to dominate. The floc size of the flocculation experiment conducted in the wheel in comparison with the jar is shown in Fig. 8. The median floc size in the wheel for all concentrations is higher than in the experiments with the jar. The reason for this difference can be attributed to the same reason that has been proposed to explain the residence time experiments: organic matter coming into contact with clay at very low shear will bind and lead to large flocs. Similarly to the resting time tests, this flocculation occurred very rapidly (within 2.5 min). After 30 min, the median floc size started reducing. An interesting observation was made when analysing the video at $5.0\,g\,L^{-1}$: flocs started to disintegrate during the settling process (see Figure S6). This is in line with the hypothesis proposed for the resting time experiments: the rearrangement of the organic material on the clay (minimizing contact with water) causes the flocs to break up.

Residence time at the bottom of a jar experiments with samples of the wheel were also conducted. The samples were collected from the wheel and transferred to jars. Although the concentration in the jars could not be well controlled, the jars were still labelled according to the concentrations used in the wheel experiments. The samples were stored at room temperature. The median floc size with different clay concentrations is shown in Fig. 9. It can be observed that there is a decrease in floc size after day 1, after which the floc size increases over time. The rate of increase in floc size is decreasing with concentration. As can be seen from the floc size distributions (Fig. 9(A–C)), all floc sizes were reduced after the first day. Again, the hypothesis is that the rearrangement of the organic material onto the clay (minimizing its contact with water) causes the flocs to break up. As for the residence time experiments with the jar tests, the later increase in particle size is attributed to the manipulation of the jars during sampling. In contrast to jar experiments, however, size growth is observed for all concentrations, which leads us to conclude that the structure of the flocs is different in this case. Most probably, flocs are overall less reconformed than in jar test experiments, leading to a larger clay surface area onto which organic matter can aggregate.

4. Conclusions

In this study, laboratory experiments were carried out to examine the flocculation of deep-sea clay collected from two different regions of CCFZ. The results showed the importance of shear, particle concentration, and organic matter in flocculation. Two types of mixing were studied: turbulent mixing in a jar and slow mixing in a rotating wheel, whereby differential settling plays a significant role. It was found that even at low mixing time (less than 2.5 min), flocculation occurs at all shear and mixing conditions, even at the lowest clay concentration used ($0.5\,g\,L^{-1}$). The flocs found had a median size that is, on average, 3–6 times larger than the median floc size of the unflocculated material. The organic matter present in the sample was found to be in the form of long strains, and sweep flocculation is likely to occur. The behaviour of median floc size at steady-state upon shear in jar test experiments led us to conclude that the organic matter present in the samples has a low affinity for both water and clay. Because of the peculiar affinity the organic matter has with water and clay, the median floc size displays the following trends:

- With flocs having experienced turbulent mixing, a shear threshold (around $125\,s^{-1}$) is required for the organic matter to uncoil and successfully bind to the clay with increased collision frequencies (i.e. with increasing shear rate), the median floc size is getting

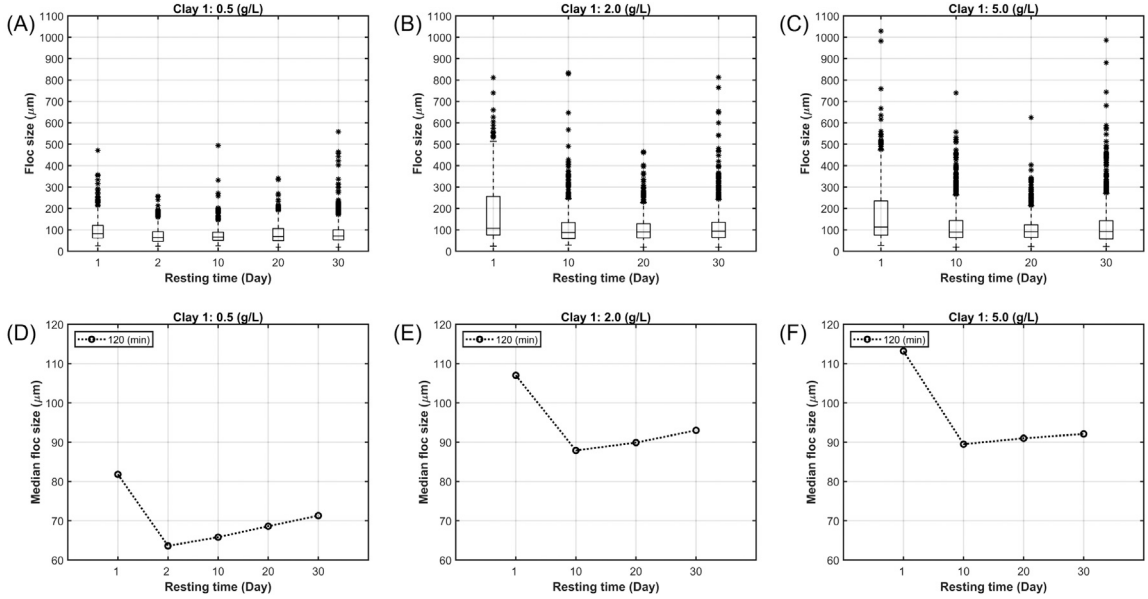

Fig. 9. Effect of resting time on floc size at different concentrations in the wheel: (A,D) $0.5\,g\,L^{-1}$, (B,E) $2.0\,g\,L^{-1}$ and (C,F) $5.0\,g\,L^{-1}$.

larger; longer mixing times result in an increase in floc size below $125\,s^{-1}$, when the median floc size is well below the Kolmogorov microscale, which reduces the break-up of flocs since flocs are then simply advected by the flow. At shear rates above $125\,s^{-1}$, the median floc size decreases with mixing time due to the breaking/reconformation of flocs.

- With flocs having experienced low mixing in the wheel, differential settling promotes flocculation, and the flocs are found to be two or three times larger than the ones formed in turbulent mixing in the jar tests. At long mixing times, floc sizes decrease, most probably due to the rearrangement of organic matter onto clay, which leads to the floc break-up.

Experiments were also performed to study the influence of the floc residence time at the bottom of the jars on their size. It was found that:

- With flocs having experienced turbulent mixing, flocs that were originally not touching one another in the jar would flocculate when put into contact by the gentle handling of the jar. Flocs that were already into contact with one another would see their median floc size decrease. This was attributed to a slow diffusion process that would lead to a rearrangement of organic matter onto the clay to maximize the contact area between organic matter and clay, leading to the breakage of flocs.
- With flocs having experienced low mixing in the wheel, flocs would, in all cases, first break and have a smaller size on day 2 compared to day 1. This was again attributed to the rearrangement of organic matter onto the clay so as to maximize the contact area between organic matter and clay, leading to a breakage of flocs. After day 2, the median flocs size increased, which was, as for the jar test experiments, linked to the handling of the jars for sampling, as floc–floc interaction is then promoted. The flocs formed by differential settling of the wheel are expected to be of a more open structure than those formed by turbulent mixing, which is why they would aggregate upon touching (whereas flocs formed in turbulent mixing would not).

These findings highlight the complexity of flocculation kinetics for natural sediments. Most flocculation studies focus on the interaction between solid particles and synthetic flocculants (like polyacrylamides) used in sanitary engineering or mining engineering. Natural flocculants, on the other hand, are quite diverse. Some of these flocculants, known as Extracellular Polymeric Substances (EPS), consist mostly of polysaccharides that are expected to perform like polyacrylamides — in the sense that they are hydrophilic and known to bind to mineral clay easily through specific surface groups, hydrogen bonds or cation bridging. However, as discussed in the article, other natural substances are amphiphilic (having a hydrophilic "head" and a hydrophobic "tails"). The results found in this article are in line with the hypothesis that the organic matter in the samples is amphiphilic, like, for instance, a phospholipid (commonly found in deep-sea areas). An analysis of the organic matter contained in the samples would be required to confirm this hypothesis.

In conclusion, the results found in the present article confirm that flocculation plays a significant role in deep-sea areas. Due to the short time scales involved, and the (at first surprising) result that flocculation increases with shear, it is expected that flocculation also plays a significant role in plumes generated by mining activities.

CRediT authorship contribution statement

W. Ali: Writing – review & editing, Writing – original draft, Visualization, Validation, Methodology, Investigation, Formal analysis. **A. Kirichek:** Writing – review & editing, Supervision, Project administration, Conceptualization. **C. Chassagne:** Writing – review & editing, Supervision, Resources, Project administration, Methodology, Funding acquisition, Conceptualization.

Declaration of competing interest

The authors declare that they have no known competing financial interests or personal relationships that could have appeared to influence the work reported in this paper.

Data availability

No data was used for the research described in the article.

Acknowledgements

This work is performed in the framework of PlumeFloc (TMW.BL.019.004, Topsector Water and Maritiem: Blauwe route) within the MUDNET academic network. The authors would also like to thank Deltares for using their experimental facilities in the framework of the MoU between TU Delft/Deltares.

Appendix A. Supplementary data

Supplementary material related to this article can be found online at https://doi.org/10.1016/j.apor.2024.104099.

References

Ali, W., Chassagne, C., 2022. Comparison between two analytical models to study the flocculation of mineral clay by polyelectrolytes. Cont. Shelf Res. (ISSN: 0278-4343) 250, 104864. http://dx.doi.org/10.1016/j.csr.2022.104864.

Ali, W., Enthoven, D., Kirichek, A., Helmons, R., Chassagne, C., 2022. Effect of flocculation on turbidity currents. Front. Earth Sci. 10, 1014170. http://dx.doi.org/10.3389/feart.2022.1014170.

Ali, W., Kirichek, A., Chassagne, C., 2023. Settling velocity as function of cohesive sediment particle concentration. Appl. Clay Sci. 2024.

Alldredge, A.L., Silver, M.W., 1988. Characteristics, dynamics and significance of marine snow. Prog. Oceanogr. (ISSN: 0079-6611) 20 (1), http://dx.doi.org/10.1016/0079-6611(88)90053-5.

BGR, 2019. Environmental Impact Assessment for the testing of a pre-protoype manganese nodule collector vehicle in the Eastern German license area (Clarion-Clipperton Zone) in the framework of the European JPI-O MiningImpact 2 research project.

Blue Nodules D1.7, 2020. Environmental Impact Assessment (EIA) components for test mining up to prototype level (TRL 6) Technical report.

Danovaro, R., Gambi, C., Dell'Anno, A., Magagnini, M., Noble, R., Tamburini, C., Weinbauer, M., 2008. Exponential decline of deep-sea ecosystem functioning linked to benthic biodiversity loss. Curr. Biol. 18, 1–8.

Deng, Z., 2022. The Role of Algae in Fine Cohesive Sediment Flocculation (Ph.D. thesis). Delft University of Technology, http://dx.doi.org/10.4233/uuid:07ed19ec-52a8-4abb-ad7f-64eaace73f3a.

Deng, Z., He, Q., Safar, Z., Chassagne, C., 2019. The role of algae in fine sediment flocculation: in-situ and laboratory measurements. Mar. Geol. 71–84, 413.

Dyer, K.R., 1989. Sediment processes in estuaries: Future research requirements. J. Geophys. Res. 94 (C10), 14327.

Elerian, B., 2023. Numerical Investigation of Turbidity Flows Generated By Polymetallic Nodules Mining (Ph.D. thesis). Delft University of Technology.

Elerian, M., Van Rhee, C., Helmons, R., 2022. Experimental and numerical modelling of deep-sea-mining-generated turbidity currents. Minerals 12 (5), 558. http://dx.doi.org/10.3390/min12050558.

Fettweis, M., Baeye, M., 2015. Seasonal variation in concentration, size, and settling velocity of muddy marine flocs in the benthic boundary layer. J. Geophys. Res. Oceans 120, 5648–5667. http://dx.doi.org/10.1002/2014jc010644.

Gage, J.D., Tyler, P.A., 1991. Deep-Sea Biology: A Natural History of Organisms At the Deep-Sea Floor. Cambridge University Press.

Gillard, B., 2019. Towards Deep Sea Mining-Impact of Mining Activities on Benthic Pelagic Coupling in the Clarion Clipperton Fracture Zone (Ph.D. thesis). Universität Bremen.

Gillard, B., Purkiani, K., Chatzievangelou, D., Vink, A., Iversen, M.H., Thomsen, L., 2019. Physical and hydrodynamic properties of deep sea mining-generated, abyssal sediment plumes in the Clarion Clipperton Fracture Zone (eastern-central Pacific). Elementa 7, 5.

Gollner, S., Kaiser, S., Menzel, L., Jones, D.O.B., Brown, A., Mestre, N.C., Oevelen, D.V., Menot, L., Cola, A., Canals, M., Cuvelier, D., Durden, J.M., Gebruk, A., Egho, G.A., Haeckel, M., Marcon, Y., Mevenkamp, L., Morato, T., Pham, C.K., Purser, A., Sanchez-vidal, A., Vanreusel, A., Vink, A., Martinez, P., 2017. Resilience of benthic deep-sea fauna to mining activities. Mar. Environ. Res. 129, 76–101.

Gratiot, N., Manning, A.J., 2004. An experimental investigation of floc characteristics in a diffusive turbulent flow. J. Coast. Res. 105–113, http://www.jstor.org/stable/25736635.

Haalboom, S., Schoening, T., Urban, P., Gazis, I.Z., de Stigter, H., Gillard, B., Baeye, M., Hollstein, M., Purkiani, K., Reichart, G.J., Thomsen, L., Haeckel, M., Vink, A., Greinert, J., 2022. Monitoring of anthropogenic sediment plumes in the clarion-clipperton zone, NE equatorial Pacific ocean. Front. Mar. Sci. 9, http://dx.doi.org/10.3389/fmars.2022.882155.

Harbour, P.R., Leitner, A.B., Ruehlemann, C., Annemiek, V., Sweetman, A.K., 2020. Benthic and demersal scavenger biodiversity in the eastern end of the clarion-clipperton zone – An area marked for polymetallic nodule mining. Front. Mar. Sci. 1–14.

Hein, J.R., Koschinsky, A., Kuhn, T., 2020. Deep-ocean polymetallic nodules as a resource for critical materials. Nat. Rev. Earth Environ. 1, 3, 158–169.

Ho, Q.N., Fettweis, M., Spencer, K.L., Lee, B.J., 2022. Flocculation with heterogeneous composition in water environments: A review. Water Res. (ISSN: 0043-1354) 213, http://dx.doi.org/10.1016/j.watres.2022.118147.

ISA, 2015. A Geological Model of Polymetallic Nodule Deposits in the Clarion-Clipperton Fracture Zone [WWW Document]. Technical Report, p. 6.

ISA, 2019. Current Status of the Reserved Areas with the International Seabed Authority [WWW Document]. Technical Report.

Jones, D.O.B., Kaiser, S., Sweetman, A.K., Smith, C.R., Menot, L., Vink, A., Trueblood, D., Greinert, J., Billett, D.S.M., Arbizu, P.M., Radziejewska, T., Singh, R., Ingole, B., Durden, J.M., Clark, M.R., Stratmann, T., Simon-lledo, E., 2017. Biological responses to disturbance from simulated deep-sea polymetallic nodule mining. PLOS ONE 12 (2), e0171750.

Kaiser, S., R. Smith, C., Martinez Arbizu, P., 2013. Editorial: Biodiversity of the clarion clipperton fracture zone. Mar. Biodiversity 47, 259–264. http://dx.doi.org/10.1007/s12526-017-0733-0.

Kranck, K., 1973. Flocculation of suspended sediment in the sea. Nature 246, 348–350. http://dx.doi.org/10.1038/246348a0.

Lang, M.A., Dasselaar, S., Aasly, K., Larsen, E., 2019. Blue nodules deliverable report d3.4 report describing the process flow overview pu. pp. 1–23.

Lee, B.J., Kim, J., Hur, J., Choi, I.H., Toorman, E., Fettweis, M., Choi, J.W., 2019. Seasonal dynamics of organic matter composition and its effects on suspended sediment flocculation in river water. Water Resour. Res. 55, 6968–6985. http://dx.doi.org/10.1029/2018WR024486.

MacIver, M.R., 2019. Safas: Sedimentation and floc analysis software. https://github.com/rmaciver/safas.

Manning, A., Friend, P., Prowse, N., Amos, C., 2007. Estuarine mud flocculation properties determined using an annular mini-flume and the labsfloc system. Cont. Shelf Res. 27 (8), 1080–1095.

Mewes, K., Mogollón, J.M., Picard, A., Rühlemann, C., Kuhn, T., Nöthen, K., Kasten, S., 2014. Impact of depositional and biogeochemical processes on small scale variations in nodule abundance in the Clarion-Clipperton Fracture Zone. Deep-Sea Res. I 91, 125–141. http://dx.doi.org/10.1016/j.dsr.2014.06.001, Elsevier.

Mietta, F., Chassagne, C., Manning, A.J., Winterwerp, J.C., 2009. In-fluence of shear rate, organic matter content, pH and salinity on mud flocculation. Ocean Dyn. 59, 5, 751–763.

Parzanini, C., Parrish, C.C., Hamel, J.F., Mercier, A., 2018. Functional diversity and nutritional content in a deep-sea faunal assemblage through total lipid, lipid class, and fatty acid analyses. PLOS ONE 13 (11), e0207395. http://dx.doi.org/10.1371/journal.pone.0207395.

Peacock, T., Alford, M., 2018. Is deep-sea mining worth it? Sci. AM 72–77. http://dx.doi.org/10.1038/scientificamerican0518-72.

Peacock, T., Ouillon, R., 2023. The fluid mechanics of deep-sea mining. Annu. Rev. Fluid Mech. 55 (2023), 403–430. http://dx.doi.org/10.1146/annurev-fluid-031822-010257.

Riemann, F., 1983. Biological aspects of deep-sea manganese-nodule formation. Oceanol. Acta 6 (3), 303–311.

Safar, Z., Rijnsburger, S., Sanz, M.I., Chassagne, C., Manning, A., Pietrzak, J., Souza, A., van Kessel, T., Horner-Devine, A., Flores, R., McKeon, M., 2019. Characterization and dynamics of suspended particulate matter in the near field of the rhine river plume during a neap tide. In: Geophysical Research Abstracts (Vol. 21).

Shakeel, A., MacIver, M.R., van Kan, P.J.M., Kirichek, A., Chassagne, C., 2021. A rheological and microstructural study of two-step yielding in mud samples from a port area. Colloids Surf. A 624, 126827.

Shakeel, A., Safar, Z., Ibanez, M., Paassen, L., Chassagne, C., 2020. Flocculation of clay suspensions by anionic and cationic polyelectrolytes a systematic analysis. Minerals 1–24.

Sujith, P.P., Gonsalves, M.J.B., 2021. Ferromanganese oxide deposits: Geochemical and microbiological perspectives of interactions of cobalt and nickel. Ore Geol. Rev. 139, 104458.

Suzumura, M., 2005. Phospholipids in marine environments: a review. Talanta 66 (2), 422–434.

Vanreusel, A., Hilario, A., Ribeiro, P.A., Menot, L., 2016. Threatened By Mining, Polymetallic Nodules are Required To Preserve Abyssal Epifauna. Nature Publishing Group, pp. 1–6.

Verlaan, P.A., Cronan, D.S., 2022. Origin and variability of resource-grade marine ferromanganese nodules and crusts in the Pacific Ocean: A review of biogeochemical and physical controls. Geochemistry 82 (1), 125741.

Volz, J.B., Mogollon, J.M., Geibert, W., Arbizu, P.M., Koschinsky, A., Kasten, S., 2018. Natural spatial variability of depositional conditions, biogeochemical processes and element fluxes in sediments of the eastern Clarion Clipperton Zone, Pacific Ocean. Deep-Sea Res. I 0–1. http://dx.doi.org/10.1016/j.dsr.2018.08.006, Elsevier Ltd.

Webb, T.J., Vanden Berghe, E., O'Dor, R., 2010. Biodiversity's big wet secret: The global distribution of marine biological records reveals chronic under-exploration of the deep pelagic ocean. PLoS One 5 (e10223).

Ye, L., Manning, A.J., Hsu, T.J., 2020. Corrigendum to oil-mineral flocculation and settling velocity in saline water. Water Res. 173, 115569.

Zawadzki, D., Macicag, L., Abramowski, T., McCartney, K., 2020. Fractionation trends and variability of rare earth elements and selected critical metals in pelagic sediment from abyssal basin of ne pacific (clarion-clipperton fracture zone). Minerals 10, http://dx.doi.org/10.3390/min10040320.